# An Algebraic Solution Method for Nonlinear Inverse Scattering

Martina T. Bevacqua, Lorenzo Crocco, *Senior Member, IEEE*, Loreto Di Donato, and Tommaso Isernia, *Member, IEEE*

***Abstract*—By using properly designed synthetic experiments and an original approximation of the contrast sources, we are able to recast the inverse scattering problem in an algebraic form (in a subset of points of the imaged domain) and hence to solve it by means of closed form formulas. The new approximation relies on the assumption that the contrast sources induced by the different synthetic experiments are focused in given points belonging to the scatterer. As such, the method involves a preprocessing step in which the outcome of the original scattering experiments is recombined into the new, virtual, ones enforcing the expected currents' behavior. Examples with numerical and experimental data are provided to assess the actual possibility of setting such a synthetic experiments framework and show the effectiveness of the proposed solution method.**

***Index Terms*— Microwave Imaging, Inverse Scattering Problem, Synthetic Experiments, Focusing, Contrast Source Approximation, Diagonalized System.**

## I. Introduction

INVERSE scattering is an active area of research in applied electromagnetics, thanks to its relevance in both theory and applications. As a matter of fact, the capability of recovering in non-invasive way information on non-accessible targets by processing the fields they scatter is indeed useful in sub-surface prospections, biomedical diagnostics and safety and security surveying operations, only to mention some examples.

On the other hand, due to the difficulty in tackling the non-linearity and ill-posedness of the inverse problem [1], the challenging task of developing effective solution methods is still an open issue. Broadly speaking, most of the efforts carried out in the literature are concerned with three different classes of approaches. *Qualitative* approaches [2] restrict the problem's scope to shape reconstruction in order to overcome non-linearity and form the image with a minimal computational effort. *Quantitative* methods such as [3-9] tackle instead the full characterization of the targets through iterative optimization. As such, they are computationally demanding and prone to the occurrence of false solutions [4,5]. Finally, *hybrid* methods also do exist (see f.i. [10]).

An interesting possibility that has recently emerged is that of developing inversion methods based on "ad hoc" experiments, designed in such a way to simplify the relationship between the unknown and the data [11, 12]. Notably, the implementation of such a concept does not require specific devices or measurement procedures, but just a re-arrangement of results arising from the actually available experiments. As such, this strategy can also be seen as a kind of an adaptive beamforming approach that preludes the actual inversion task and reduces its complexity. Examples of such a strategy include [12], where the decomposition of the time reversal operator is exploited to synthetically shape the waveform of a multi-view radar depending on the imaged targets, and [11], where the information resulting from a qualitative preprocessing is exploited to define synthetic experiments in which a linearization of the scattering phenomenon is possible (beyond the traditional Born or Extended Born approximations validity).

In this paper, we present a new inversion method based on a synthetic experiments framework. While the idea in [11] was to enforce specific features of the field, we here consider the possibility of "conditioning" the contrast source, that is, the current induced in the targets, by the probing incident fields. In particular, the proposed method relies on induced currents that are synthetically focused in a set of "pivot" points belonging to the imaged domain.

A key point of the proposed approach is the introduction of a novel analytical approximation for the peculiar kind of currents at hand which holds true in a neighborhood of the pivot point. Such an approximation allows to express the (focused) current in terms of the contrast function, and hence permits to recast the inverse problem in such a way that the values of the contrast in the pivot points can be achieved by solving a diagonalized system of (third degree) algebraic equations. The unknown properties of the whole imaged region are then achieved by simply interpolating the obtained results. As a consequence, provided the proposed approximation holds true, the inverse scattering problem is solved by means of closed form formulas, and, hence, in a

This is the postprint reviewed version of the following article: Bevacqua, M.T.; Crocco, L.; Di Donato, L.; Isernia, T., "An Algebraic Solution Method for Nonlinear Inverse Scattering," IEEE Transactions on Antennas and Propagation, vol.63, no.2, pp. 601-610, Feb. 2015. Article has been published in final form at: http://ieeexplore.ieee.org/document/6987259.

reliable and extremely fast manner.

As shown through examples, the proposed method is capable of imaging targets that were so far only tackled by means quantitative inversion tools which are both computationally demanding and prone to false solutions [4,5].

Of course, for the method to work properly, it is necessary to understand the conditions for which the approximation is viable, and outline a strategy to design the required synthetic experiments. Both these aspects are addressed in detail in the paper, which is organized as follows. In Section II, we cast the inverse scattering problem, outline the synthetic experiments framework, and show how they can be used to condition the contrast source. In Section III, assuming that synthetic experiments capable to induce a focused current are available, we introduce the new approximation, while in Section IV the new inversion procedure suggested from the adopted contrast source expansion is introduced and described. Finally, in Section V, we devise a way to set in practice the required synthetic experiments and assess the capabilities of the proposed method through numerical examples. Conclusions follow.

Throughout the paper we consider the canonical 2D scalar problem (TM polarized fields) and we assume and drop the time harmonic factor $exp\{j\omega t\}$.

## II. Statement of the Problem

### A. Formulation of the inverse scattering problem

Let us consider an unknown nonmagnetic object, embedded in a homogeneous medium of electromagnetic features $\mu_b$ and $\varepsilon_b$ and conductivity $\sigma_b$, with compact support $\Omega$. At the frequency $\omega$, the scatterer is probed by means of a set of incident fields transmitted by some antennas located in the far-field of $\Omega$ on a closed curve $\Gamma$. Without loss of generality, we assume that the resulting scattered fields are measured by receiver antennas also located on $\Gamma$. The equations describing the scattering problem for the generic $v$ -th incident field are:

$$E_{scat}{}^{(v)}(\boldsymbol{r}) = k^2 \int_{\Omega} G(\boldsymbol{r},\boldsymbol{r}')\, W^{(v)}(\boldsymbol{r}')d\boldsymbol{r}' = \mathcal{A}_e\left[W^{(v)}\right], \quad \boldsymbol{r} \in \Gamma \tag{1}$$

$$W^{(v)}(\boldsymbol{r}) = \chi(\boldsymbol{r})E_{inc}{}^{(v)}(\boldsymbol{r}) + \chi(\boldsymbol{r})\, k^2 \int_{\Omega} G(\boldsymbol{r},\boldsymbol{r}')\, W^{(v)}(\boldsymbol{r}')d\boldsymbol{r}' = \chi E_{inc}{}^{(v)} + \chi\mathcal{A}_i\left[W^{(v)}\right], \quad \boldsymbol{r} \in \Omega \tag{2}$$

where $\boldsymbol{r} = (\boldsymbol{x},\boldsymbol{y})$ and $E_{inc}{}^{(v)}(\cdot)$, $E_{scat}{}^{(v)}(\cdot)$ and $W^{(v)}(\cdot)$ are the incident field, scattered field and contrast source induced in $\Omega$, respectively, $k = \omega\sqrt{\mu_b\varepsilon_b}$ is the wavenumber in the host medium, $G(\boldsymbol{r},\boldsymbol{r}')$ is the Green's function pertaining to the homogeneous background and $\mathcal{A}_e$ and $\mathcal{A}_i$ are a short notation for the integral radiation operators.

The unknown contrast function, $\chi(\cdot)$ relates the electromagnetic features of the object and host medium and it is defined as:

$$\chi(\boldsymbol{r}) = \frac{\varepsilon_s(\boldsymbol{r}) - j\sigma_s(\boldsymbol{r})/(\omega\varepsilon_0)}{\varepsilon_b(\boldsymbol{r}) - j\sigma_b(\boldsymbol{r})/(\omega\varepsilon_0)} - 1 \tag{3}$$

where $\varepsilon_s$ and $\sigma_s$ are the relative permittivity and electric conductivity of the scatterer, respectively.

In the inverse scattering problem the aim is to estimate the contrast function from the measured scattered fields. Note the problem is non linear, as the contrast sources also depend on the unknown contrast. A second fundamental limitation that has to be faced is the bounded amount of non-redundant information that one can collect, so that only a finite number of independent probing fields (and measurements) can be actually exploited in the inversion [13].

### B. The Synthetic Experiments Framework

Due to the linearity of the scattering phenomenon (and Maxwell equations) with respect to the primary sources, if one recombines the incident fields with known coefficients $\alpha_v$, a scattered field is obtained, which is the superposition (with the same coefficients) of the corresponding scattered fields.

More in detail, if

$$E_{inc,s}(\boldsymbol{r}) = \sum_{v=1}^{N} \alpha_v\, E_{inc}(\boldsymbol{r},\vartheta_v) \tag{4}$$

is the considered superposition of the incident fields, then:

$$W_s(\boldsymbol{r}) = \sum_{v=1}^{N} \alpha_v\, W(\boldsymbol{r},\vartheta_v) \tag{5.a}$$

$$E_{scat,s}(\varphi) = \sum_{v=1}^{N} \alpha_v\, E_{scat}(\vartheta_v,\varphi) \tag{5.b}$$

are the corresponding contrast source and scattered field, respectively. In (4) and (5), $\vartheta_v$ and $\varphi$ denote the generic incidence direction and the generic observation one, respectively.

Hence, re-arranging the original experiments allows to build new experiments. We will refer to these experiments as "synthetic" experiments. In fact, they do not require additional physical measurements (and the subscript *s* stands in fact for "synthetic").

Of course, the amount of information carried by the synthetic experiments cannot exceed that of the original ones, and actually some information can be lost, if they are not carefully designed. On the other side, which is the reason of their interest, properly designed synthetic experiments can give rise to total fields or contrast sources exhibiting (or approaching) some given behavior. Hence, when recasting the inverse scattering problem in terms of the synthetic experiments, the exploitation of such properties can be used to pursue, in a more convenient and simple way, the solution of the problem.

## III. A New Approximation for the Contrast Source

Let us assume we have been able to design a set of synthetic experiments that induce currents having a focused distribution around given "pivot" points $\boldsymbol{r}_p$. Notably, this is a feasible goal, as the problem of focusing an electromagnetic wave in an unknown environment has been largely addressed in the literature. In particular, adaptive time reversal procedures [14], strategies exploiting the linear sampling method (LSM) [2,15,16] or convex optimization [17] represent some of the most effective and widely adopted procedures. Hence, we can assume to have exploited one of the abovementioned procedures to determine the suitable coefficients $\alpha_v$.

Moreover, let us make the additional assumption that the contrast function is slowly variable around each pivot point, so that one can consider the medium to be approximately homogeneous in a neighborhood of $\boldsymbol{r}_p$.

By exploiting canonical solutions [18] in a reference system centered on the pivot point, the contrast source can be expressed as a superposition of Bessel functions, i.e.:

$$W_s^{(p)}(\boldsymbol{r}) = \sum_{n=-\infty}^{+\infty} a_n J_n(k_p \rho)\, e^{jn\left(\phi - \frac{\pi}{2}\right)} \tag{6}$$

where $\phi$ and $\rho$ are the polar coordinates with respect to $\boldsymbol{r}_p$, $a_n$ is an amplitude coefficient, $J_n(\cdot)$ is the Bessel function of order $n$ and $k_p = k\sqrt{1+\chi_p}$ and $\chi_p$ are, the "local" wavenumber and "local" values of contrast in $\boldsymbol{r}_p$ (and its neighborhood), respectively.

Observing that the induced current at hand is focused, and remembering the behavior of Bessel functions in the origin, it follows that the only term which survives in (6) in a neighborhood of the pivot point is the one with $n = 0$. As a result, in such a neighborhood we can approximate the actual contrast sources by means of the zero order Bessel function, whose argument depends on the unknown properties of the medium in $\boldsymbol{r}_p$, i.e.,:

$$W_s^{(p)}(\boldsymbol{r}) \approx a_0 J_0(k_p|\boldsymbol{r}-\boldsymbol{r}_p|), \qquad \boldsymbol{r}_p \in \Omega, \qquad \boldsymbol{r} \in \mathcal{I}_{R_p}(\boldsymbol{r}_p) \tag{7}$$

where $\mathcal{I}_{R_p}(\boldsymbol{r}_p)$ is a circular neighborhood of $\boldsymbol{r}_p$ of radius $R_p$.

Then, advantage can be taken from the Multiplication Theorem [19] for Bessel functions, according to which:

$$\varepsilon^{-\nu} J_\nu(\varepsilon z) = \sum_{n=0}^{\infty} \frac{1}{n!}\left[\frac{(1-\varepsilon^2)z}{2}\right]^n J_{\nu+n}(z) \tag{8}$$

so that:

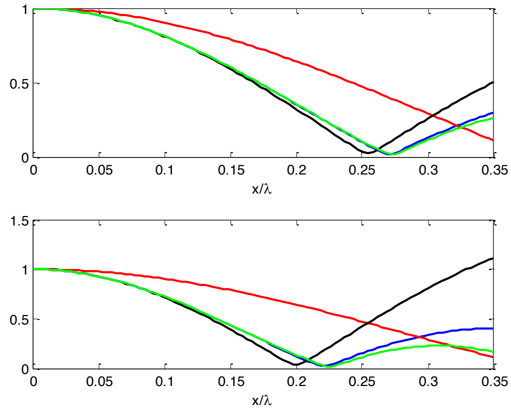


Fig. 1. Behavior of the Bessel function amplitude (blue curve) as compared to the approximation (9) truncated at the first term (red curve), at the second term (black curve) and at the third term (green curve). Two complex contrast values are reported: in the upper panel $\chi_v = 1 - 0.05i$, while in the lower one $\chi_v = 2 - 0.1i$. The background medium is lossless.

$$J_0(k_p|\boldsymbol{r}-\boldsymbol{r}_p|) = \sum_{n=0}^{\infty} \frac{1}{n!}\left(\frac{-\chi_p k|\boldsymbol{r}-\boldsymbol{r}_p|}{2}\right)^n J_n(k|\boldsymbol{r}-\boldsymbol{r}_p|) \tag{9}$$

Expression (9) has a two-fold interest.

First, it provides an expression that accounts for both the radiating and non-radiating components of the contrast source [20], in the considered neighborhood. In fact, according to [20], radiating (minimum energy) components of a source have to fulfill the Helmholtz equation in the background medium, so that the first term of (9) can be identified as the radiating component, while the remaining terms are the non-radiating ones.

Second, as we are considering a neighborhood of $\boldsymbol{r}_p$, we can truncate (9) to the first few terms, so that it is possible to rewrite (7) as follows:

$$\begin{aligned} W_s^{(p)}(\boldsymbol{r}) \approx a_0^{(p)} \Big\{ & J_0(k|\boldsymbol{r}-\boldsymbol{r}_p|) \\ & - \frac{1}{2}\chi_p\, k|\boldsymbol{r}-\boldsymbol{r}_p| J_1(k|\boldsymbol{r}-\boldsymbol{r}_p|) \\ & + \frac{1}{8}\chi_p^2 \left(k|\boldsymbol{r}-\boldsymbol{r}_p|\right)^2 J_2(k|\boldsymbol{r}-\boldsymbol{r}_p|)\Big\} \end{aligned} \tag{10}$$

where now the argument of the Bessel functions just depends on the background medium.

Eq.(10) is a remarkable result, as it provides (within the validity of the approximation resulting from the truncation) an explicit algebraic relationship between $\chi_p$ and $W_s^{(p)}$, which is linear if the expansion is truncated to the second term, and quadratic otherwise.

Of course, (10) has a limited validity, which depends on the distance $\rho = |\boldsymbol{r}-\boldsymbol{r}_p|$ from the pivot point, as well as from the local value of the contrast. As expected, (see also fig.1) the larger $\rho$ (and the higher is $\chi_p$), the smaller the range of validity of the approximation (10).

As $\chi_p$ is the unknown of the problem, the determination of the actual geometric neighborhood of validity is not trivial (see Section IV for further discussion). However, in the proximity of the pivot point it is possible to express the contrast source as an algebraic function of the contrast, times a scalar variable ($a_0$). As shown in the following, this circumstance provides the basis to introduce a new and effective inversion method.

## IV. A New Algebraic Solution Procedure

To show how the approximation introduced in the previous Section leads to a new and effective inversion, let us first rewrite the scattering equations with respect to the relevant synthetic experiments framework. In particular, eq. (2) can be rewritten as:

$$W_s{}^{(p)}(\boldsymbol{r}) = \chi(\boldsymbol{r}) E_{inc,s}{}^{(p)}(\boldsymbol{r}) + \chi(\boldsymbol{r})\, k^2 \int_{\mathcal{I}_{R_p}} G(\boldsymbol{r},\boldsymbol{r}')\, W_s{}^{(p)}(\boldsymbol{r}') d\boldsymbol{r}' + \chi(\boldsymbol{r})\, k^2 \int_{\bar{\mathcal{I}}_{R_p}} G(\boldsymbol{r},\boldsymbol{r}')\, W_s{}^{(p)}(\boldsymbol{r}') d\boldsymbol{r}' \quad (11)$$

where, as we are using approximations (7) and (10), the domain $\Omega$ has been divided in two non-overlapping subdomains: the neighborhood $\mathcal{I}_{R_p}$ of $\boldsymbol{r}_p$ and its complementary set with respect to $\Omega$, $\bar{\mathcal{I}}_{R_p}$. As long as the currents induced by the synthetic experiments are well focused, and $\mathcal{I}_{R_p}$ is properly chosen, it is possible to neglect the second integral (see also subsection C below).

Similarly, eq. (1) can be split into two contributions:

$$E_{scat,s}{}^{(p)}(\boldsymbol{r}) = k^2 \int_{\mathcal{I}_{R_p}} G(\boldsymbol{r},\boldsymbol{r}')\, W_s{}^{(p)}(\boldsymbol{r}') d\boldsymbol{r}' + k^2 \int_{\bar{\mathcal{I}}_{R_p}} G(\boldsymbol{r},\boldsymbol{r}')\, W_s{}^{(p)}(\boldsymbol{r}') d\boldsymbol{r}' \quad (12)$$

where the second term at the right hand side can be again neglected.

### *A. A new inversion procedure*

By means of the explicit relationship between the contrast source and the contrast arising from (10), and following the analytical developments reported in the Appendix, it is possible to particularize and merge eqs.(11) and (12) for each pivot point into the single third order algebraic equation:

$$\bar{A}^{(p)} {\chi_p}^3 + \bar{B}^{(p)} {\chi_p}^2 + \bar{C}^{(p)} \chi_p + \bar{D}^{(p)} = 0 \quad (13)$$

where the only unknown is the value of the contrast in the considered pivot point. In fact, (see Appendix) the scalar variable $a_0$ can also be expressed in terms of the contrast.

Eq.(13) is the core of the new inversion method, as it allows to estimate the unknown contrast in the pivot point at hand by solving a cubic equation, which admits, as well known, a closed form solution [21]. Hence, it is possible to obtain the required estimate in a very efficient way, without resorting to iterative methods.

To estimate the overall contrast, one can consider all the pivot points for which the synthetic experiments have been designed, so that the overall inverse scattering problem can be formulated as a (diagonal) system of polynomial equations:

$$A(\mathrm{X} \odot \mathrm{X} \odot \mathrm{X}) + B(\mathrm{X} \odot \mathrm{X}) + C\mathrm{X} + D = 0 \quad (14)$$

where $\odot$ denotes the Hadamard product between vectors, $X = [\chi_1 \cdots \chi_k \cdots \chi_P]^T$ is the vector that contains the punctual values of the unknown contrast in the selected pivot points $\boldsymbol{r}_p$, and $(\,)^T$ denotes the matrix transposition. Finally, $A$, $B$, $C$ and $D$ are diagonal matrices given by:

$$A = \begin{bmatrix} \bar{A}^{(1)} & \cdots & 0 \\ \vdots & \ddots & \vdots \\ 0 & \cdots & \bar{A}^{(\mathrm{P})} \end{bmatrix} \quad (15.a)$$

$$B = \begin{bmatrix} \bar{B}^{(1)} & \cdots & 0 \\ \vdots & \ddots & \vdots \\ 0 & \cdots & \bar{B}^{(\mathrm{P})} \end{bmatrix} \quad (15.b)$$

$$C = \begin{bmatrix} \bar{C}^{(1)} & \cdots & 0 \\ \vdots & \ddots & \vdots \\ 0 & \cdots & \bar{C}^{(\mathrm{P})} \end{bmatrix} \quad (15.c)$$

$$D = \begin{bmatrix} \bar{D}^{(1)} & \cdots & 0 \\ \vdots & \ddots & \vdots \\ 0 & \cdots & \bar{D}^{(\mathrm{P})} \end{bmatrix} \quad (15.d)$$

and the expression of the different elements can be found in the Appendix.

The solution of (14) provides the values of the contrast function in the $P$ considered pivot points. Then, an interpolation is performed to obtain the image of the reconstructed contrast over the investigated region. In particular, a linear interpolation is adopted in the following because of the assumed slow spatial variations of the contrast.

### *B. Managing false solutions*

The inversion method described above is extremely effective and efficient, and it has the unique feature of allowing to solve the non-linear inverse scattering problem through simple algebraic tools.

The achieved equations still preserve the non-linearity of the problem, while allowing to deal with a kind of diagonalized (or localized) problem. Notably, diagonalization and algebraic nature also allow to manage in an effective fashion the false solutions problem [5, 22]. In fact, the third degree polynomial considered in the method admits three roots, so that two of them correspond to "false solutions". In the canonical case of targets embedded in free space (dealt with in the assessment given in Section V), these roots are expected to be spaced (in the average) of 120°, so that only one of them is physically realizable (i.e, only one root will have a positive real part and a negative imaginary part). In addition, a priori information concerned with the expected "slow" spatial variability of the contrast can be possibly exploited. Similar "physical feasibility" arguments are expected to hold in more general cases.

### *C. On the Choice of $R_p$ and of the order of Bessel Expansions*

The choice of $R_p$ has to obey a very obvious trade off. In fact, from one side, one needs a value of $R_p$ as large as possible, as this will reduce the error arising from neglecting the second term in (11) and (12). On the other side, large values of $R_p$ may imply lack of validity of both (7) and (10). Notably, as already stated, the "optimal" choice of $R_p$ also depends on the value of $\chi_p$, which is unknown.

By taking advantage of the very fast inversion allowed by the obtained diagonalized algebraic formulation, we adopt in the following an "a posteriori" criterion to choose a suitable value of $R_p$ for all pivot points. In particular, after using several trial values for $R_p$, we quantify a posteriori the fitting which is achieved in the scattering equations (using the contrast functions as estimated from the different choices of the radius). To this end, we introduce the residual:

$$Res = \sum_p \frac{\left\| {W_s}^{(p)} - \chi {E_{inc,s}}^{(p)} + \chi \mathcal{A}_i\left[{W_s}^{(p)}\right] \right\|^2}{\left\| {E_{inc,s}}^{(p)} \right\|^2} \tag{16}$$

where $\chi$ and ${W_s}^{(p)}$ are the contrast and the contrast sources obtained for a given radius $R_p$. In particular, ${W_s}^{(p)}$ is evaluated as in equation (7), where ${a_0}^{(p)}$ is calculated by averaging with respect to the different measurements, as shown in the Appendix.

To set $R_p$, the residual (16) is appraised for different tentative values (belonging to a limited range), as well as for second and third order expansions of the Bessel function (see eq. 10) Then, the value corresponding to the minimum residual error is picked as the most appropriate one. It is worth to remark that although this a posteriori evaluation requires solving the system (14) for each tentative radius value, the procedure is obviously very fast, as the tentative solutions are still computed in a closed form. Moreover, this operation is intrinsically parallel.

## V. Method's Implementation and Assessment

The inversion method presented in the previous Section and based on the contrast source approximation and expansion is composed of three steps:

- the design of "ad hoc" synthetic experiment to condition the induced currents;
- the solution of the diagonal system to estimate the contrast function in the pivot points;
- the linear interpolation to obtain the image of the reconstructed contrast over the investigated region.

As previously mentioned, there are several strategies to implement the first step. Among the possible choices, we adopt in the following a procedure based on the LSM [2]. The reason for this choice is due to the fact that, besides providing the information required to recombine the induced currents in such a way that they are focused in a pivot point [15], the LSM also provides information on the target's support, which is useful to properly locate the pivot points in which the approximated contrast source expansion is cast.

As a consequence of all the above, the specific implementation (of the general strategy) which is assessed in the following can only be used in situations where both LSM and the adopted approximations hold valid. Nevertheless, as we are going to show, these situations actually include cases that have only been solved (up to now) with computationally onerous iterative methods.

### *A. Simulated data*

We have first carried out a "controlled" assessment with simulated data. In these examples, one or more unknown objects are positioned inside a square domain of side L and, following [13], the same number of receivers and transmitters, both located on a circumference Γ of radius R, has been considered, $\mathrm{N} = \mathrm{M} = 2\,\Re\mathrm{e}[\mathrm{k}]\mathrm{L}/\sqrt{2}$. The scattered field data, simulated by means of a full-wave forward solver based on the method of moments, have been corrupted with a random Gaussian noise with given SNR.

To evaluate the accuracy of the retrieved contrast function, we use the normalized mean square error defined by:

$$err = \frac{\|\chi - \tilde{\chi}\|^2}{\|\chi\|^2} \tag{17}$$

where $\chi$ is the actual contrast profile and $\tilde{\chi}$ the estimated one.

The first example deals with a lossless circular cylinder, see figure 2.(a), with $\varepsilon_s = 2$, $\mathrm{L} = 1.5\lambda$. Following [23], a number of cells $N_c$ equal to $64 \times 64$ has been used, while $\mathrm{N} = \mathrm{M} = 15$, $\mathrm{SNR} = 20$ dB and $\mathrm{R} = 3\lambda$.

First, the target support has been estimated from the LSM indicator [2,11,15] over the imaged domain (see fig. 2.(b)). In particular we compute logarithmic LSM indicator, (as the logarithm allows to emphasize the energy variation amongst the different pivot points), and then normalized it over the whole imaged domain. Then, the pivot points have been uniformly spread over the estimated support (see fig. 2.(b)), and the coefficients pertaining to the LSM solutions in the selected pivot points have been used to define the synthetic experiments. Finally, the diagonal system of third degree algebraic equations has been solved, adopting the criteria in

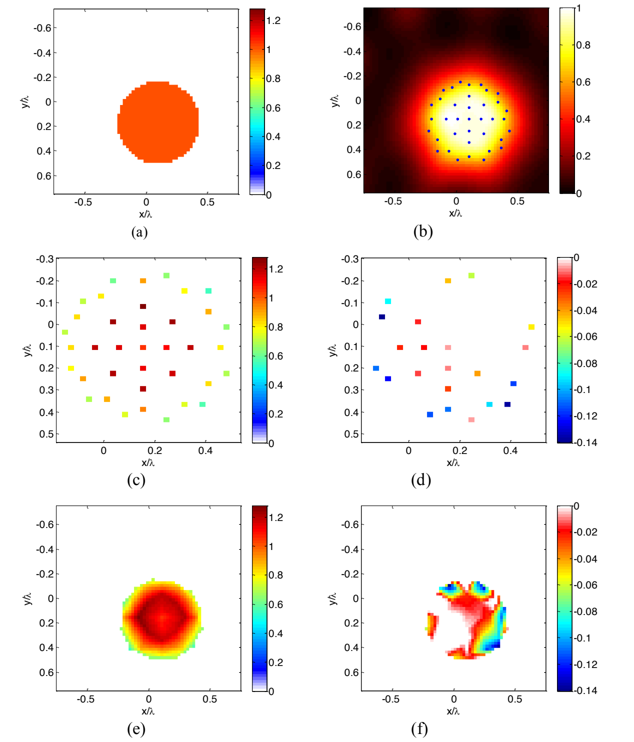

Fig. 2. The circular homogeneous target: (a) real part of the reference profile; (b) Normalized logarithmic LSM indicator map with the selected pivot points superimposed as dots; (c) real part and (d) imaginary part of punctual value of retrieved contrast, before interpolation; (e) real part and (f) imaginary part of retrieved contrast.

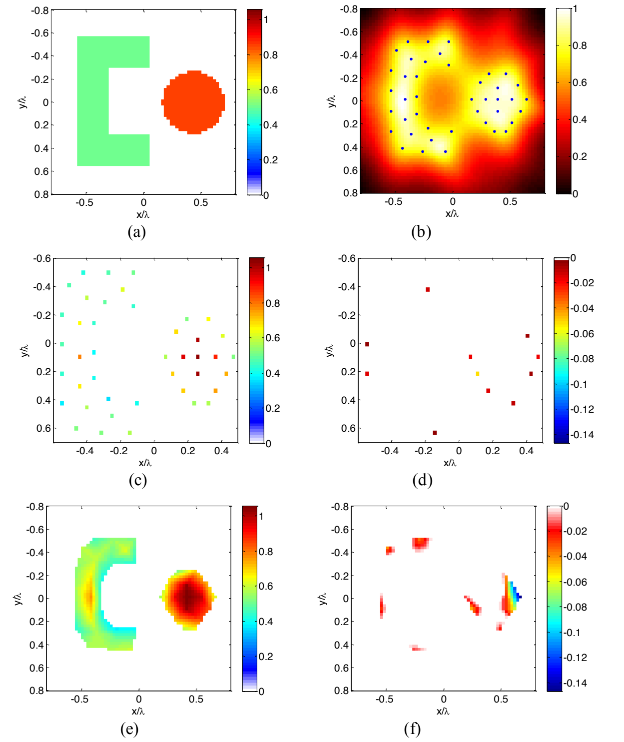

Fig. 3. The C-O target: (a) real part of the reference profile; (b) Normalized logarithmic LSM indicator with the selected pivot points superimposed as dots; (c) real part and (d) imaginary part of punctual value of retrieved contrast, before interpolation; (e) real part and (f) imaginary part of retrieved contrast.

Section IV.B to choose the "physically feasible" root in each pivot point. The real and imaginary parts of the obtained contrast values are shown in figs 2(c) and (d), respectively. Note that the value of the imaginary parts in some pivot points is thresholded to zero in order to guarantee both the expected slow variability and the physical feasibility condition (i.e. $\mathfrak{Im}\,\{\chi\} <= 0$).

The retrieved contrast function, resulting from the linear interpolation of the punctual values estimated in the selected pivot points (figs 2(c)-(d)), is shown in figs 2(e)-(f). As it can be seen, the real part is accurately estimated and the lossless nature envisaged (as the imaginary part is indeed negligible with respect to the real one). In the proximity of the scatterer contour, the contrast is slightly underestimated, because of the reduced capability of the LSM to focalize the currents. The final reconstruction error is as low as 8%.

In the second example, we have considered a more complex profile consisting of two lossless scatterers with different electromagnetic features (fig. 3(a)): a C-shape target with $\varepsilon_s = 1.5$, and a circular target with $\varepsilon_s = 1.85$. In this case, $N_c = 64 \times 64$, $N = M = 17$, $R = 1.6\lambda$, $L_D = 1.6\lambda$. Finally, the simulated data used for processing has been affected by a simulated error with SNR=20 dB. As it can be noted from figs 3(e)-(f), a quite accurate reconstruction, corresponding to $err = 34\%$, is achieved.

## B. *Experimental data*

While the previous examples show the implementation and the feasibility of the proposed method, in this subsection we assess its performance with some of the experimental data-set provided by the Institute Fresnel of Marseille, France [24, 25], typically adopted to benchmark inverse scattering procedures. Interestingly, to the best of our knowledge, both the data set considered in the following have been so far successfully tackled only using iterative inversion procedures and multiple frequency data (see for instance [26] and [10] for the two cases, respectively). Hence, the capability of successfully handling them by means of the proposed approach and with monochromatic data is indeed very significant.

As compared with the previous examples using simulated data, the Fresnel experiments introduce the additional difficulty of dealing with a partially aspect limited configuration. As a matter of fact, Fresnel targets are probed by primary sources which completely surround them, but, for each source position, the fields are measured by moving the receiving probe along a 240° arc, excluding the 120° degree angular sector centered on the source position [24, 25]. In each example the incident field has been estimated according to the fitting procedure described in [26].

First, we have considered the *TwinDiel* data set [24],

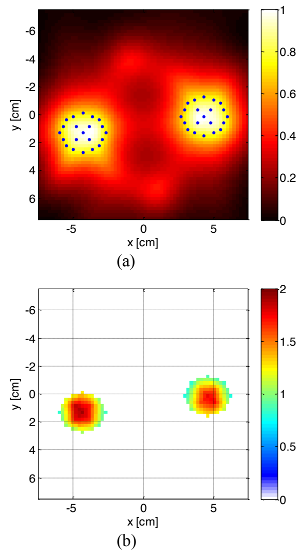


Fig. 4. The *TwinDiel* Fresnel dataset: (a) Normalized logarithmic LSM indicator with the selected pivot points superimposed as dots; (b) real part of retrieved contrast.

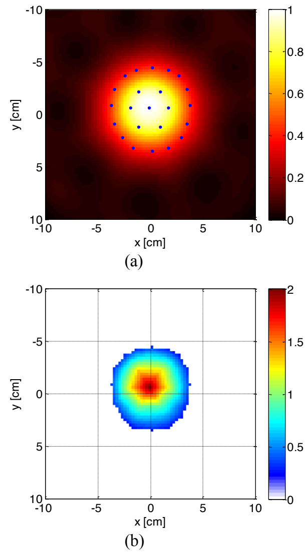


Fig. 5. The *FoamDielInt* Fresnel dataset: (a) Normalized logarithmic LSM indicator with the selected pivot points superimposed as dots; (b) real part of retrieved contrast.

consisting of two identical circular dielectric cylinders with radius 1.5 cm and relative permittivity $3 \pm 0.3$. In this dataset, the original number of illumination directions is 36, while the original number of measurements is 49 for each view. Moreover, in this experiment the investigated domain is a square of side 0.15 m and the working frequency is 4 GHz. The normalized logarithmic LSM indicator is shown in fig. 4(a). Such a result is achieved by adopting as data matrix a $72 \times 36$ matrix in which the original data entries that are not available are replaced with zeroes. Again, the LSM indicator is exploited to choose the pivot points and define the virtual experiments.

Fig. 4(b) shows the real part of the retrieved contrast, while the imaginary part (which is not displayed) turns out to be negligible. As it can be seen, the proposed method achieves a satisfactory reconstruction while using a non-iterative computationally simple solution procedure.

Second, we have considered the *FoamDielInt* target [25], which is an inhomogeneous object, constituted by two nested circular cylinders: an outer one made of foam (radius 40 mm, relative permittivity $\varepsilon_r \approx 1.45$) that hosts another circular cylinder made of berylon (radius 15 mm and $\varepsilon_r = 3$). This target represents an extremely challenging case for the proposed approach, as the contrast profile exhibits an abrupt discontinuity of the electromagnetic features, thus violating the assumption underlying the approximation introduced in Section III. The data set exploited for this example has been supplied by the Institute Fresnel and is constituted by 72 incident fields and 61 receivers per view. In this case, the working frequency is 3 GHz and the side of the investigated area is 0.20 m. The result, reported in fig. 5(b), has been achieved by adopting a $45 \times 36$ multiview-multistatic data matrix obtained by means of an under sampling of the original data in which the entries not available are replaced with zeros. As can be seen, despite the above mentioned difficulties, the proposed method is able to accurately image the unknown target. Note that in this case the selection of the pivot points has been performed using both the LSM indicator's map and the estimate of the radius of the minimum circle enclosing the target. This latter is obtained by exploiting the spectral properties of the scattered field data [27], according to which the target is expected to be enclosed in a circle of radius 6cm.

## VI. Conclusions

In this paper, we have introduced a new inverse scattering procedure based on suitably designed synthetic experiments and a new approximation of the contrast sources. In particular, the original experiments have been re-organized into new synthetic ones so to focus the resulting "synthetic" contrast sources in given points belonging to the scatterer. Then, the contrast currents have been approximated by means of Bessel functions of zero order and, finally, expanded according to the Bessel function's Multiplication theorem. This step represents the core of the approach, as it allows to recast the inverse problem through a diagonal system of algebraic equations. Hence, the contrast function can be estimated by means of the solution of third degree equations. Notably, a tuning of the underlying approximations (using an a posteriori criterion) is also usefully exploited.

The applicability of this approach depends on the limitations of the preprocessing step, as well as on the validity of the approximations used on the contrast sources. As such, the proposed quantitative inversion method is expected to largely exceed the range of effectiveness of the traditional weak scattering approximations.

Examples dealing with both simulated and experimental data fully confirm such an expectation. In particular, the results obtained processing Fresnel experimental data demonstrate the capability of the approach to successfully image targets without even taking advantage of frequency diversity, as usually done in the literature [26]. Moreover, although the formulation of the proposed inversion approach requires a slowly varying contrast function, results with experimental data have shown that it is possible to go beyond this assumption (or at least to successfully deal with piece-wise homogeneous targets).

Another important aspect of the proposed method is the very low computational burden it requires. As a matter of fact, it is possible to solve an algebraic third degree equation in a closed form, so that for each $R_p$ the solution is achieved in real time. Moreover, the LSM pre-processing here considered in the first step only entails the computation of the singular value decomposition [6,15] of a matrix whose size is in the order of data ($N \times M$).

Future work will aim at improving the method exploiting some recent results presented in the literature, which have introduced an improvement in the capability of estimating the shape of the unknown targets [28] and also the possibility of improving the focusing synthesized via LSM by resorting to an ex-post constrained convex optimization [17]. Furthermore, future work will also aim at exploiting the method, or better its underlying concepts, in the more challenging 3D vectorial scenario, where its features would become even more important.

## APPENDIX

Let us substitute eq.(10) in eq.(12). By neglecting the integral over $\bar{\mathcal{I}}_{R_p}$ one obtains:

$$E_{scat,s}{}^{(p)} \approx a_0{}^{(p)}\{bb^{(p)} + cc^{(p)}\chi_p + dd^{(p)}\chi_p{}^2\} \tag{A.1}$$

where:

$$bb^{(p)} = \mathcal{A}_e[J_0(k|\boldsymbol{r}-\boldsymbol{r}_p|)]$$
$$cc^{(p)} = \mathcal{A}_e\left[-\frac{1}{2}k|\boldsymbol{r}-\boldsymbol{r}_p|\,J_1(k|\boldsymbol{r}-\boldsymbol{r}_p|)\right]$$
$$dd^{(p)} = \mathcal{A}_e\left[\frac{1}{8}k^2|\boldsymbol{r}-\boldsymbol{r}_p|^2\,J_2(k|\boldsymbol{r}-\boldsymbol{r}_p|)\right]$$

Note that the operator $\mathcal{A}_e$ in (A.1) is defined over $\mathcal{I}_{R_p}(\boldsymbol{r_p})$. Moreover, since the contrast is assumed to be constant in $\mathcal{I}_{R_p}(\boldsymbol{r_p})$, it has been singled out from the integral operators. Note in (A.1), $\boldsymbol{r}$ belongs to the measurement domain.

For a given pivot point, the coefficient $a_0{}^{(p)}$ in (A.1) is constant, as it does not depend on the measurement position. As such, for each pivot point, it is possible to obtain an explicit expression for it, by averaging (A.1) with respect to the different measurements. In particular, a very compact expression for the reciprocal of $a_0{}^{(p)}$ is obtained as:

$$\frac{1}{a_0^{(p)}} \approx \{\bar{b}^{(p)} + \bar{c}^{(p)}\chi_p + \bar{d}^{(p)}\chi_p{}^2\} \tag{A.2}$$

where:

$$\bar{b}^{(p)} = \frac{1}{M}\sum_{i=1}^{M}\frac{bb^{(p)}(i)}{E_{scat,s}{}^{(p)}(i)}$$
$$\bar{c}^{(p)} = \frac{1}{M}\sum_{i=1}^{M}\frac{cc^{(p)}(i)}{E_{scat,s}{}^{(p)}(i)}$$
$$\bar{d}^{(p)} = \frac{1}{M}\sum_{i=1}^{M}\frac{dd^{(p)}(i)}{E_{scat,s}{}^{(p)}(i)}$$

Let us now substitute equation (10) in equation (11). Similarly, the algebraic equation obtained is the following one:

$$\alpha^{(p)}\chi_p{}^3 + \beta^{(p)}\chi_p{}^2 + \gamma^{(p)}\chi_p + \delta^{(p)} = 0 \tag{A.3}$$

where:

$$\alpha^{(p)} = \frac{1}{8}a_0{}^{(p)}\mathcal{A}_i\left[k^2|\boldsymbol{r}-\boldsymbol{r}_p|^2\,J_2(k|\boldsymbol{r}-\boldsymbol{r}_p|)\right]$$
$$\beta^{(p)} = -\frac{1}{2}a_0{}^{(p)}\mathcal{A}_i[k|\boldsymbol{r}-\boldsymbol{r}_p|\,J_1(k|\boldsymbol{r}-\boldsymbol{r}_p|)]$$
$$\gamma^{(p)} = E_{inc,s}{}^{(p)} + a_0{}^{(p)}\mathcal{A}_i[J_0(k|\boldsymbol{r}-\boldsymbol{r}_p|)]$$
$$\delta^{(p)} = -a_0{}^{(p)}$$

If now one uses the equation (A.2) in equation (A.3), a final third degree polynomial expression can be obtained, where the only unknown is the contrast. In fact:

$$\bar{A}^{(p)}\chi_p{}^3 + \bar{B}^{(p)}\chi_p{}^2 + \bar{C}^{(p)}\chi_p + \bar{D}^{(p)} = 0 \tag{A.4}$$

where:

$$\bar{A}^{(p)} = E_{inc,s}{}^{(p)}\bar{d}^{(p)} + \frac{1}{8}\mathcal{A}_i\left[k^2|\boldsymbol{r}-\boldsymbol{r}_p|^2\,J_2(k|\boldsymbol{r}-\boldsymbol{r}_p|)\right]$$
$$\bar{B}^{(p)} = E_{inc,s}{}^{(p)}\bar{c}^{(p)} - \frac{1}{2}\mathcal{A}_i[k|\boldsymbol{r}-\boldsymbol{r}_p|\,J_1(k|\boldsymbol{r}-\boldsymbol{r}_p|)]$$
$$\bar{C}^{(p)} = E_{inc,s}{}^{(p)}\bar{b}^{(p)} + \mathcal{A}_i[J_0(k|\boldsymbol{r}-\boldsymbol{r}_p|)]$$
$$\bar{D}^{(p)} = -1$$

Equation (A.4) is a third degree polynomial equation in the only unknown $\chi_p$. Therefore, its resolution allows to obtain the local value of the contrast in each pivot point.

## ACKNOWLEDGEMENT

The authors thank Dr. A. Litman and Dr. J.-M. Jeffrin from Institute Fresnel of Marseille, France for providing the inhomogeneous target data-set.

## REFERENCES


[1] D. Colton and R. Kress. “Inverse Acoustic and Electromagnetic Scattering Theory”, *Springer-Verlag,* Berlin, Germany, 1998.

[2] F. Cakoni and D. Colton. “Qualitative methods in inverse scattering theory”, *Springer-Verlag*, Berlin, Germany, 2006.

[3] M. Pastorino, “ Microwave Imaging”, *John Wiley*, New York, May 2010.

[4] T. Isernia, V. Pascazio, and R. Pierri. “A nonlinear estimation method in tomographic imaging”, *IEEE Trans. Geosci. Remote Sens.*, 35:910-923, 1997.

[5] T. Isernia, V. Pascazio, and R. Pierri. “On the local minima in a tomographic imaging technique”, *IEEE Trans. Geosci. Remote Sens.*, 39:1596-1607, 2001.

[6] M. Bertero and P. Boccacci. “Introduction to Inverse Problems in Imaging”, Institute ofPhysics, Bristol, UK, 1998.

[7] A. Abubakar and P V. van den Berg “Iterative forward and inverse algorithms based on domainintegral equations for three-dimensional electric and magnetic objects”, *J. Comp. Phys*. 195236–62, 2004.

[8] L. Crocco and T. Isernia, “Inverse scattering with real data: detecting and imaging homogeneous dielectric objects”, *Inverse Probl.*, 17(6):1573, 2001.

[9] Scapaticci, R.; Catapano, I.; Crocco, L., "Wavelet-Based Adaptive Multiresolution Inversion for Quantitative Microwave Imaging of Breast Tissues", *IEEE Trans. Antennas Propag.*, 60(8):3717-3726, Aug. 2012.

[10] Catapano, I.; Crocco, L.; D'Urso, M.; Isernia, T., "On the Effect of Support Estimation and of a New Model in 2-D Inverse Scattering Problems", *IEEE Trans. Antennas Propag.*, 55(6):1895-1899, June 2007.

[11] L. Crocco, I. Catapano, L. Di Donato and T. Isernia, “The linear sampling method as a way to quantitative inverse scattering”, *IEEE Trans. Antennas Propag.*, 60(4) 1844-1853, Apr. 2012.

[12] Bellomo, L.; Belkebir, K.; Saillard, M.; Pioch, S.; Chaumet, P., "Inverse scattering using a Time Reversal RADAR", *Electromagnetic Theory (EMTS), 2010 URSI International Symposium on*, pp.381,384, 16-19 Aug. 2010.

[13] O. M. Bucci and T. Isernia, “Electromagnetic inverse scattering: Retrievable nformation and measurement strategies”, *Radio Sci.*, 32:2123–2138, 1997.

[14] De Rosny, J., G. Lerosey, and M. Fink, “Theory of electromagnetic time-reversal mirrors”, *IEEE Trans. Antennas Propag*., 58(10):3139-3149, 2010.

[15] I. Catapano, L. Crocco, and T. Isernia. “On simple methods for shape reconstructionof unknown scatterers”, *IEEE Trans. Antennas Propag.*, 55:1431-1436, 2007.

[16] L. Crocco, L. Di Donato, D. A. M. Iero, T. Isernia, “An adaptive method to focusing in unknown scenario”, *Progress in Electromagnetic Research*, 130: 563-579, 2012.

[17] L. Crocco, L. Di Donato, D. A. M. Iero, T. Isernia, “A New Strategy for Constrained Focusing in Unknown Scenarios", *IEEE Antenn. and Wirel. Pr.*, 11:1450-1453, 2012.

[18] D. S. Jones, “Acoustic and Electromagnetic Waves”, *Oxford, England: Clarendon Press*, 1986.

[19] Abramowitz M.; Stegun I. A. “Handbook of Mathematical Functions with Formulas, Graphs, and Mathematical Tables”, *New York, Dover Publications*, 1964.

[20] Marengo, E. A. and R. W. Ziolkowski, “Nonradiating and minimum energy sources and their fields: Generalized source inversion theory and applications”, *IEEE Trans. Antennas Propag*., 48(6):1553-1562, 2000.

[21] G. Cardano, “Artis Magnae Sive de Regulis Algebraicis, Liber Unus”, 1545 (see *G. Cardano,* “Ars Magna or the Rule of Algebra”*, Dover Publications, Paperback,* 1993*).*

[22] T. Isernia, F. Soldovieri, G. Leone and R. Pierri “On the local minima in phase reconstruction algorithms”, *Radio Sci.,* 32(6):1887-1899, 1996.

[23] J. Richmond, “Scattering by a dielectric cylinder of arbitrary cross section shape”, *IEEE Trans. Antennas Propag*., 13(3):334-341, 1965.

[24] K. Belkebir and M. Saillard, “Special section: Testing inversion algorithms against experimental data”, *Inverse Probl.*, 17:1565–2028, 2001.

[25] K. Belkebir and M. Saillard, “Special section: Testing inversion algorithms against real data: Inhomogeneous targets”, *Inverse Probl.*, 21, 2005.

[26] L. Crocco and T. Isernia, “Inverse scattering with real data: Detecting and imaging homogeneous dielectric objects”, *Inverse Probl.*, 17(6):1573, 2001.

[27] L. Crocco, M. D'Urso and T. Isernia, "Testing the contrast source extended born method against real data: The TM case," *Inverse Probl.*, 21(6):S33-S50, 2005.

[28] Crocco, L., Di Donato, L., Catapano, I., Isernia, T., “An Improved Simple Method for Imaging the Shape of Complex Targets", *IEEE Trans. Antennas Propag*., 61(2):843-851, Feb. 2013.